Similarity solution for low Mach number spherical shocks

B. E. McDonald
Naval Ocean Research and Development Activity, NSTL, Mississippi 39529

J. Ambrosiano
Berkeley Research Associates, Springfield, Virginia 22150

(Received 29 May 1988; accepted for publication 16 June 1988)

A nonlinear progressive wave equation (NPE) describes the evolution of a low Mach number shock wave. The NPE is the nonlinear time domain counterpart of the frequency domain linear parabolic wave equation (PE) for small angle propagation. The NPE in spherical symmetry admits a similarity solution that specifies both the shape of the pulse and the shock strength as a function of range. For finite amplitude spherical waves whether self-similar or not, the theory predicts constancy of an impulse integral corresponding to that of linear theory. For the self-similar waves, theory and available data are in qualitative agreement in the following areas: (1) The shock strength decreases with range as an approximate power law; (2) the temporal behavior of the solution at fixed range is a shock discontinuity followed by a roughly exponential decay; and (3) the effective relaxation time behind the shock is in reasonable agreement with data for slightly more than the first decade in range.

PACS numbers: 43.25.Cb

INTRODUCTION

A number of sources give rise to waves that spend much or all of their lifetimes as "weak" shocks, propagating only slightly faster than Mach 1. These sources include supersonic aircraft,[1] underwater explosions,[2,3] and a number of laboratory experiments and procedures. A shock is considered mathematically weak when the density of the medium changes by a small amount (say, 20% or less) across the shock front. Underwater shocks are almost always weak, even though overpressures may be as high as thousands of atmospheres. If overpressure is used to measure the strength of the shock, it is important to keep in mind that, for water, the relevant scale for comparison is not ambient pressure as in the case of a gas, but bulk modulus $= \rho_0 c_0^2 \simeq 22 \times 10^3$ atm. Here, ρ_0 and c_0 are the density and linear sound speed of water.

Experimental data from underwater detonation of high-explosive charges reveal an empirical power law dependence of the shock strength (i.e., overpressure) versus range from the source.[4] Pressure relaxation times $\tau_p = |p\ (\partial p/\partial t)^{-1}|$ behind the shock front also fall with somewhat more scatter about an approximate power law in range. Specifically, peak overpressures and relaxation times for underwater explosions vary with a scaled range coordinate according to

$$p_{\max} = 0.024 \rho_0 c_0^2 (W^{1/3}/r)^{1.13}, \qquad 0.4 \lesssim r/W^{1/3} \lesssim 400 \text{ m kg}^{-1/3},$$
$$\tau_p = 92.5 \times 10^{-6} W^{1/3} (r/W^{1/3})^{0.22}, \qquad 0.4 \lesssim r/W^{1/3} \lesssim 40 \text{ m kg}^{-1/3}, \tag{1}$$

where r is the distance from the explosion in meters, W is the TNT equivalent mass of the explosive charge in kilograms, and τ_p is in seconds. Overpressures from a number of shots involving different explosive charges fall within about $\pm 20\%$ of the power law over approximately 3 decades in the scaled range.[2] Relaxation time data are subject to more scatter than the overpressure data. The scatter about the power law (1) for relaxation time is approximately $\pm 30\%$.

The scaling of range by $W^{1/3}$ in (1) is easily explained by dimensionality considerations. When a point source dumps hydromechanical energy E impulsively and symmetrically into an infinite homogeneous medium whose pressure is negligible, the only macroscopic scale size inherent to the configuration is $L_0 = (E/\rho_0 c_0^2)^{1/3}$, referred to by Sedov[5] as the dynamic range. Here, L_0 is an order-of-magnitude estimate for the shock radius at a time when the root-mean-squared fluid particle speed falls below c_0. The energy E is proportional to the mass W of the explosive, so that scaling to L_0 implies scaling to $W^{1/3}$. The scaling of τ_p by $W^{1/3}$ reflects the inherent time scale L_0/c_0.

The approximate power law behavior of the overpressure and relaxation time with range is not so obvious. The simplicity of the range dependence of data summarized by (1) does, however, suggest some sort of similarity behavior in the evolution of the shock wave. Similarity solutions have long been known to be relevant to strong shocks,[5,6] but assumptions regarding the dominance of the shock over the ambient medium fail as the shock grows weak.

Rogers[2] presented a semiempirical theory whose numerical solution reproduced approximately the $r^{-1.13}$ power law for overpressure versus range. The range behavior of the relaxation time from this theory was, however, less satisfying. The predicted relaxation time increased too rapidly with range close to the source and then too slowly far from the source. The empiricism in this method lay in imposing the assumption (with some support from available data) that, just after the passage of the shock past a fixed range point, the temporal behavior of the overpressure was an exponential falloff. Actually, this behavior can hold only for a limited time, for the density profile must change sign at some point in order to conserve mass. This will be discussed further below. The solution method of Ref. 2 employed a one-di-

mensional method of characteristics immediately behind the shock, followed by an approximate adaptation to spherical symmetry.

In contrast, the method used here begins with a reduced nonlinear wave equation accurate to second order in the density perturbation. A formal similarity solution is extracted in which time and range dependence enter through a single variable c_0t/r. Our results show a more rapid dropoff of overpressures near the source than Rogers' predictions. The relaxation time prediction from our theory is in better agreement with data at close ranges, but also flattens off far from the source.

I. THE NONLINEAR PROGRESSIVE WAVE EQUATION (NPE)

The propagation of three-dimensional finite amplitude acoustic pulses subject to refraction, diffraction, and nonlinear steepening is described by a nonlinear progressive wave equation (NPE) derived in a related article.[7] The NPE has been shown[8] to be the nonlinear time domain equivalent of the frequency domain parabolic wave equation (PE).[9] The NPE for a spherical nonlinear wave in a homogeneous medium is

$$\frac{\partial R}{\partial t} = -c_0\left(\frac{\partial}{\partial r}+\frac{1}{r}\right)(R+\beta R^2)+O\left(R^3,\frac{R^2}{r}\right), \quad (2)$$

where

$$R=\rho_1/\rho_0. \quad (3)$$

Here, ρ_1 is the density perturbation, and

$$\beta = 1+\frac{\rho_0}{2c_0^2}\frac{\partial^2 p}{\partial p^2}\bigg|_0 = 1+\frac{\partial \log c}{\partial \log \rho}\bigg|_0. \quad (4)$$

In Eq. (4) β is a thermodynamic quantity referred to as the medium's coefficient of nonlinearity. For a perfect gas with specific heat ratio γ, $\beta=(1+\gamma)/2$. The value of β for water is approximately 3.5. The derivatives in (4) are taken from an adiabatic equation of state for the medium. This is permissable in our model, since for a weak shock, heating (entropy increase as opposed to adiabatic compression) is proportional to the cube of the density jump.[10] An estimate of the smallness of shock heating can be obtained from Table 2.1 of Cole[3] for a water shock of overpressure $\Delta p = 5000$ atm (an approximate upper limit to the region of applicability of our model). Immediately behind the shock, the total temperature increase (adiabatic compression plus entropy generated at the shock) ΔT is approximately 5 °C. Values for $T\Delta S$ reveal that, upon return to atmospheric pressure, the water is heated by only about 1.3 °C. We maintain that this reflects comparison of a cubic to a quadratic effect when $\Delta p/\rho_0 c_0^2 \simeq 0.25$. (The fact that the constant of proportionality in this comparison is near unity is fortuitous.)

Equation (2) describes the evolution of a finite amplitude compressional wave in the farfield of a spherical source. Inherent in the derivation of the nonlinear term in (2) is the assumption that it applies to a wave whose gradient scale size at a point is much less than the radius r from the origin. In the absence of the nonlinear term, (2) describes *exactly* outgoing spherical wave solutions

$$R = f(r-c_0t)/r \quad (5)$$

of the linear wave equation in spherical symmetry:

$$\frac{\partial^2 R}{\partial t^2} = c_0^2\nabla^2 R. \quad (6)$$

In this solution, mass conservation relies on a consistency condition referred to as the conservation of impulse:

$$\int f(x)dx \equiv \int rR\,dr = 0. \quad (7)$$

The integration limits in (7) extend over the entire range where f is nonzero. The second form of this condition will be shown also to apply to nonlinear spherical waves. Since Eq. (2) retains only linear and quadratic terms, the assumption of constant β allows β to be absorbed into a scaled density perturbation

$$s=\beta\rho_1/\rho_0. \quad (8)$$

The resulting equation for s is then

$$\frac{\partial s}{\partial t} = -c_0\left(\frac{\partial}{\partial r}+\frac{1}{r}\right)\phi(s), \quad (9)$$

where

$$\phi(s) = s+s^2/2.$$

An immediate result of (9) is that the location of a continuous zero crossing ($s=0$) propagates at a speed c_0.

II. SIMILARITY SOLUTION

A similarity solution to (9) may be found by combining the independent variables r and t into a single independent variable c_0t/r. A solution is sought in the form

$$s=s(\eta), \quad \eta = c_0t/r. \quad (10)$$

Substituting (10) into (9) leads to

$$\left(\eta\frac{d\phi}{ds}-1\right)\frac{ds}{d\eta} = \phi(s). \quad (11)$$

The nonlinear partial differential equation (9) is thus converted to an ordinary differential equation for a restricted class of solutions of the form (10). Equation (11) may be integrated for general $\phi(s)$ by interchange of dependent and independent variables to yield

$$\eta = -\phi(s)\int\frac{ds}{\phi(s)^2}. \quad (12)$$

For $\phi(s)$ as given in (9), (12) becomes

$$\eta = 1+s+s(1+s/2)\log[|\alpha s|/(s+2)], \quad (13)$$

where α is a constant of integration. Equation (13) implicitly defines s as a function of η, i.e., the self-similar overdensity profile as a function of range and time. Equation (13) gives $\eta\to 1$ as $s\to 0$, leading to a zero crossing at $r=c_0t$ for all α.

III. SHOCK PROPAGATION

We seek solutions describing shock jumps with an undisturbed medium ahead of the discontinuity and the continuous profile (13) behind it (or between discontinuities in the case of an N wave shock). We must show that the jump conditions at the shock can be satisfied by the similarity variables in a consistent way. The form of Eq. (9) is such that results of shock physics can be applied directly. Assuming a

discontinuity between values to the left and right of the shock (denoted by subscripts l and r), the requirement of mass conservation across the shock specifies the speed at which the shock front propagates (i.e., the Rankine–Hugoniot relation):

$$\frac{dr_s}{dt} = c_0 \frac{\phi_r - \phi_l}{s_r - s_l} = c_0\left(1 + \frac{s_s}{2}\right). \tag{14}$$

The second expression in (14) assumes that the shock is a jump from $s = 0$ to $s = s_s$. The subscript s denotes evaluation on the nonzero side of the shock. The above equations allow evaluation of time derivatives of r_s, η_s, and s_s as algebraic functions of the similarity variables and time. From (10) and (14),

$$\frac{d\eta_s}{dt} = \frac{\eta_s}{t}\left[1 - \left(1 + \frac{s_s}{2}\right)\eta_s\right]. \tag{15}$$

From (11) and (15), we have

$$\frac{ds_s}{dt} = \left(\frac{ds}{d\eta}\right)_s \frac{d\eta_s}{dt}$$
$$= -\frac{s_s}{t}\left(1 + \frac{s_s}{2}\right)\eta_s\left(1 - \frac{s_s}{2(1 + s_s - \eta_s^{-1})}\right). \tag{16}$$

At this point, the similarity solution is conceptually complete. If one is given a physical overdensity field corresponding to a self-similar weak shock at an instant of time, η_s is the radius of the zero crossing behind the shock divided by the radius of the shock; s_s is determined by the overdensity at the shock according to (8), and t is the radius of the zero crossing divided by c_0. The constant of integration could be determined by solving (13) for α, substituting the known values for s_s and η_s. From this point forward, the shock jump can be integrated forward in time using (16). At any future time, the shock profile as a function of range would be specified by (13) from the zero crossing $r = c_0 t$ out to the shock radius, $r_s = c_0 t/\eta_s$, with $s = 0$ for $r > r_s$.

For comparison of results predicted here with data, it remains to give an expression for the density relaxation time behind the shock, $\tau_s = -s(\partial s/\partial t)^{-1}|_s$. From equations (9)–(11),

$$\tau_s = -s\left(\frac{ds}{d\eta}\frac{\partial \eta}{\partial t}\right)^{-1}\Big|_s$$
$$= -t\frac{s}{\eta}\frac{d\eta}{ds}\Big|_s = t\frac{\eta^{-1} - 1 - s}{1 + s/2}\Big|_s. \tag{17}$$

This gives the *density* relaxation time, whereas comparisons are to be made with *pressure* data. The conversion factor for translating density to pressure relaxation time is $\partial \log \rho_1 / \partial \log p_1$, taken adiabatically from the equation of state.

The time coordinate can be eliminated from (14) and (16) to yield an equation in which the shock radius is the independent variable:

$$\frac{d\log s_s}{d\log r_s} = \frac{r_s}{s_s}\frac{ds_s}{dt}\Big/\frac{dr_s}{dt} = -\frac{1 - \eta(1 + s/2)}{1 - \eta(1 + s)}\Big|_s. \tag{18}$$

The right-hand side of (18) involves only similarity variables, so that from (18) and (13) one can construct the overdensity versus range relation. The result can then be expressed as overpressure via the equation of state.

IV. ASYMPTOTIC BEHAVIOR FOR SMALL OVERDENSITY

To demonstrate that (18) leads to an approximate power law relation, we truncate (13) at first order in s and substitute into (18) to find

$$\frac{d\log s_s}{d\log r_s} = -1 + \frac{1}{2\log|\alpha s_s/2| + 4} + O(s_s). \tag{19}$$

Anticipating that the constant α is of order unity, the denominator on the right-hand side of (19) is a large negative number for small s, and the right-hand side is of the form $-1 - \epsilon$, where ϵ is a small, slowly varying positive quantity. Thus an approximate power relation between overdensity and range is to be expected. In the limit of small s, (19) leads to

$$s_s \simeq \text{const}\ r_s^{-1}|\log s_s|^{-1/2}. \tag{20}$$

Since s_s and r_s are approximately inversely proportional, the logarithm on the right-hand side of (20) can be replaced to read

$$s_s \simeq \text{const}\ r_s^{-1}[\log(r_s/r_0)]^{-1/2}, \tag{21}$$

where r_0 is an arbitrary constant. This asymptotic behavior recovers a well-known result.[3,11]

V. PLANAR FORM: *N* WAVES

The planar equivalent of Eq. (11) yields a solution that can be shown to satisfy the Euler equations exactly, and agree with an assumed adiabatic equation of state through second order in the overdensity. For a plane wave, the $1/r$ term is absent from (9) and, as a result the right-hand side in (11) is zero. Removing a factor $ds/d\eta$ (i.e., ruling out the trivial solution $s = \text{constant}$), Eq. (11) becomes an algebraic expression whose only solution is

$$\eta\frac{d\phi}{ds} = 1$$

or

$$s = \eta^{-1} - 1$$

or

$$\rho = \rho_0[1 + (r - c_0 t)/\beta c_0 t]. \tag{22}$$

At any given time, the spatial form of the density perturbation is a linear ramp. When the ramp has a zero crossing midway between shock discontinuities of opposing sign, the result is an *N* wave.

The following procedure can be used to show that (22) satisfies the fluid equations to the stated accuracy. Equation (22) for the density can be substituted into the mass continuity equation, allowing a direct integration for the mass flux ρv. The mass flux and density can then be substituted into the momentum equation, allowing integration for the pressure. The result is in agreement with a perfect gas law with error cubic in ρ_1.

Shock parameters for the planar similarity solution are easily integrated from (22) and (15). The shock range r_s,

shock jump s_s, and relaxation time τ_s behind the planar shock are

$$r_s = c_0(t + bt^{1/2}),$$
$$s_s = bt^{-1/2}, \tag{23}$$
$$\tau_s = bt^{1/2}/(1 + bt^{-1/2}),$$

where b is an arbitrary constant. In the planar solution, the shock overdensity is predicted to fall off as approximately the inverse square root of range, while the relaxation time behind the shock is predicted to increase approximately with the square root of range.

VI. CONSERVATION PROPERTIES

A. Mass integral

Mathematical conservation properties result from Eqs. (9) and (14) for *any* solution $s(r,t)$. These properties were not maintained nor discussed in the previous similarity theory for weak shocks.[2] This point does not invalidate that theory, it having been based on empirical observation.

In applying the mathematical solution given here to physical systems, one must bear in mind the caveat that negative fluid pressure cannot exist. A negative density perturbation can exist only to the extent that the total pressure remains non-negative. Density perturbations below this limit in water would indicate regions containing cavitation bubbles.

The plane-wave solution (22) and (23) possesses a mass integral:

$$M_{pw} = \int_{c_0 t}^{r_s} s(r,t)\, dr = \frac{c_0 b^2}{2}. \tag{24}$$

Mass fluctuations ahead of and behind the zero crossing at $r = c_0 t$ are separately conserved. This follows straightforwardly from Eqs. (22) and (23). Spherical wave solutions of Eq. (9), however, do not explicitly conserve mass for two reasons. The first is the omission of high-order terms in extracting Eq. (2) from the Euler equations. The second and more basic reason is the consistency condition (7) on outgoing spherical wave solutions of the *linear* wave equation discussed earlier. The spherical analog of (24) is

$$M_{sph} = 4\pi \int_{r_1}^{r_2} r^2 s(r,t)\, dr, \tag{25}$$

where a continuous profile is assumed between shocks at r_1 and r_2. Outside (r_1,r_2), s is taken to be zero. Continuous nonlinear pulses are tactily included in this discussion by allowing that the magnitude of the shock jumps at r_1 and/or r_2 may be zero.

Let us consider a solution $s(r,t)$ which may or may not be self-similar and calculate from (9) and (14) the time derivative of M_{sph}:

$$\dot{M}_{sph} = 4\pi r^2 \dot{s}\Big|_{r_1}^{r_2} + 4\pi \int_{r_1}^{r_2} r^2 \frac{\partial s}{\partial t}\, dr$$
$$= 4\pi c_0 \int_{r_1}^{r_2} r\phi(s)\, dr = 4\pi c_0 \int_{r_1}^{r_2} r\left(s + \frac{s^2}{2}\right) dr. \tag{26}$$

In analogy with the linear consistency condition (7), mass conservation requires the last integral on the right-hand side to be zero. Physically, if a wave is generated that does not satisfy the integral condition, it will respond by producing a trailing disturbance that offsets the imbalance. The next section shows that mass conservation depends upon impulse conservation, just as in the linear case.

B. Impulse conservation

Equation (9) possesses an integral of the motion for any solution $s(r,t)$, which is a generalization of the linear impluse integral (7). The result should be viewed as an exact result of an approximate equation, so that, in fact, it gives a quantity that is conserved to second order in the density perturbation. Defining

$$I = \int_{c_0 t}^{r_s} rs\, dr, \tag{27}$$

where r_s denotes *either* r_1 or r_2 above, Eqs. (9) and (14) give

$$\dot{I} = \dot{r}_s r_s s_s + \int_{c_0 t}^{r_s} r \frac{\partial s}{\partial t}\, dr$$
$$= c_0 r_s \left(s_s + \frac{s_s^2}{2}\right) - c_0 \int_{c_0 t}^{r_s} \frac{\partial}{\partial r} r\left(s + \frac{s^2}{2}\right) dr = 0. \tag{28}$$

In (27) and (28), it is not necessary to specify whether r_s is greater than or less than $c_0 t$. The result is that integrals ahead of and behind $r = c_0 t$ are conserved *separately*. Thus, even allowing for the dissipation implicitly present at a shock front, the integral (27) remains constant for a spherically expanding shock to second order in the overdensity. Continuous profiles are included by admitting a shock jump of zero.

With this result, it is now possible to give the condition for mass conservation analogous to (7) for linear waves. In (26), r_1 and r_2 refer to locations of shock jumps of opposing sign with a continuous profile crossing zero in between. If the integral (27) for the positive portion of the profile exactly offsets that for the negative portion, then the integral of the linear term in the last line of (26) is zero for all time. The quadratic term in (26) must now be considered. The limits of integration r_1 and r_2 can be shown to differ by an amount that scales roughly with the magnitude of s. This can be argued directly from (14). [More convincingly for self-similar solutions, the discussion of Fig. 1 below reveals that $r_s - c_0 t \simeq r_s (2.5 s_s)^{0.83}$ over much of the domain of interest.] Then, the integral of the quadratic term in the last line of (26) scales roughly as the *cube* of the amplitude of s. Thus, when

$$\int_{r_1}^{r_2} rs\, dr = 0, \tag{29}$$

mass is conserved to within the accuracy of the reduced wave equation, (9) i.e., to second order in the overdensity. Eq. (29) is the proper generalization of (7). In fact, they both can be stated in the form (29), provided that the limits of integration for linear wave propagation be interpreted not as shock locations, but as limits outside which the density perturbation is zero.

VII. RESULTS

Figure 1 gives the similarity solution (13) for three values of the constant of integration α. The particular values 0.5, 0.7, and 0.9 were chosen to fit relaxation time data as

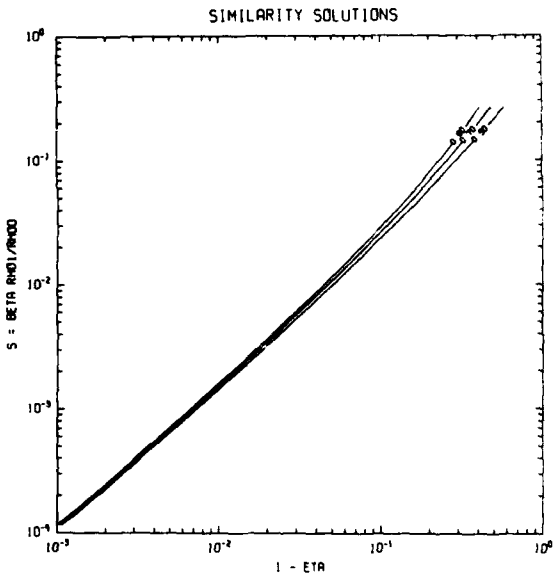

FIG. 1. Scaled density perturbation s as a function of $\eta = c_0 t / r$ from Eqs. (8) and (13). Curves are labeled with the values of α used. Log–log format reveals an approximate power law relation between s and $(1 - \eta)$.

discussed below, and to illustrate the sensitivity of experimental measurables to profile changes. For s values between roughly 10^{-4} and 10^{-2}, an approximate power law relation exists with $s \sim 0.4\,(1-\eta)^{1.2}$.

The overpressure versus range is integrated numerically from (18) with η given in terms of s in (13). Two free parameters must be specified: the pressure level at the initial range point and α in (13). In Fig. 2, the result for the overpressure versus range is given, with the initial pressure set to a value that gives reasonable agreement with Eq. (1). Pressures are calculated from an equation of state truncated after second order in s:

$$\frac{p_1}{\rho_0 c_0^2} = \frac{s}{\beta} + (\beta - 1)\left(\frac{s}{\beta}\right)^2, \tag{30}$$

where β is taken to be 3.5 for water. Shown also in Fig. 2 are results from Rogers' theory.[2] Our theory gives higher pressures at close ranges than Eq. (1) This is reasonable since overpressures should fall off faster than (1) at close ranges.

Figure 3 gives pressure–time series at a fixed range from Eq. (13) for $c_0 = 1530$ m/s. These curves do reflect an approximate exponential decay after the shock discontinuity, in agreement with observations. It is apparent that the energy and momentum in the shock increase as a α decreases. In an actual explosion, the nature of the overdensity profile produced would depend on the details of the energy release process and would likely involve the Mach number of the shock front while the shock is still strong.

In Fig. 4, pressure relaxation times versus range are given from the following expression derived from Eqs. (17) and (30):

$$\tau_- = \tau_s \frac{\partial \log s}{\partial \log p_1} = \tau_s[1 - (1 - \beta^{-1})s] + O(s^2). \tag{31}$$

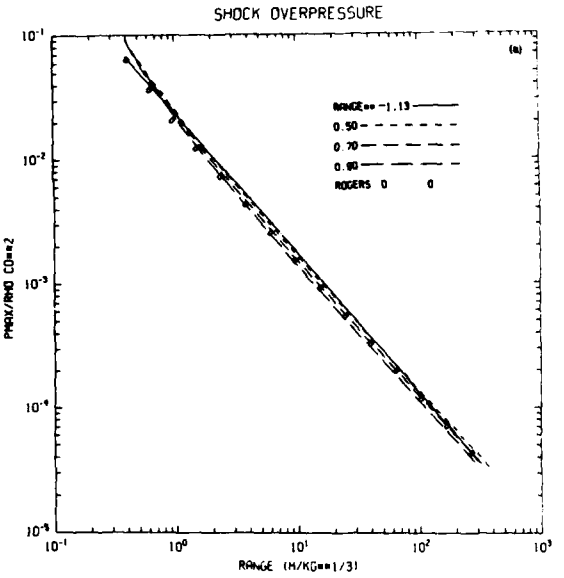

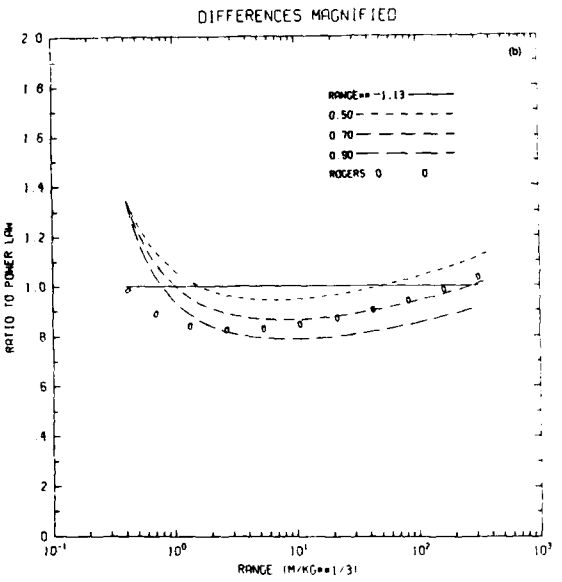

FIG. 2. Shock pressure versus range from the empirical power law (1); from numerical integration of (13), (18), and (30) (labels given in the legend are the α values used); and from Rogers' theory[2]: (a) log–log plot; (b) semilog plot to magnify differences.

Higher-order terms are estimated to change this result by less than 4%, which is much less than experimental uncertainty. Agreement with data is better than Rogers' theory[2] predicted at close ranges. This appears paradoxical, since Rogers' result for peak pressure is closer to the data in this region. Both theories do, however, tend to flatten out and underpredict the data at higher ranges. One likely explanation for departure from data is that a real explosion in general would not produce an initially self-similar profile, but such a profile could evolve over a finite propagation path. The data shown in Fig. 4 are gathered from three sources, as

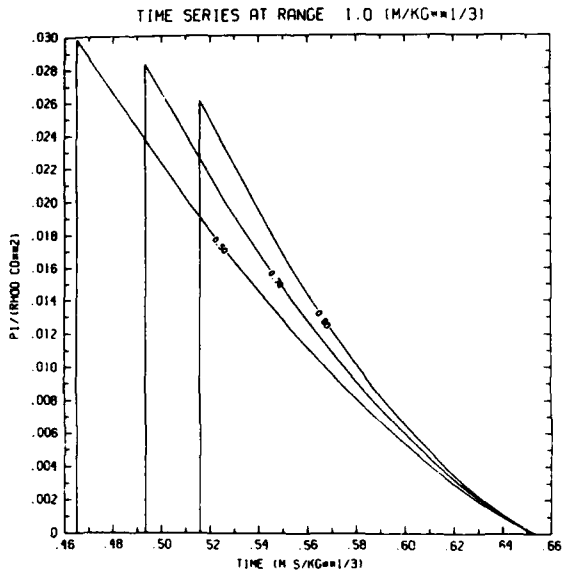

FIG. 3. Pressure–time series at fixed range as computed from (13) and (30) for the specified values of α, with p_{max} taken from the result of Fig. 2.

indicated. It is unfortunate that no one data set covers more than a factor of approximately 25 in scaled range. The similarity solution for $\alpha = 0.7$ fits the Cole data set reasonably, but the two Arons data sets are not described particularly well by any of the theoretical models, and in fact, seem to disagree with each other. Thus the behavior of the relaxation time at long ranges remains only partially understood.[12] This could indicate mechanisms not included in the theory.

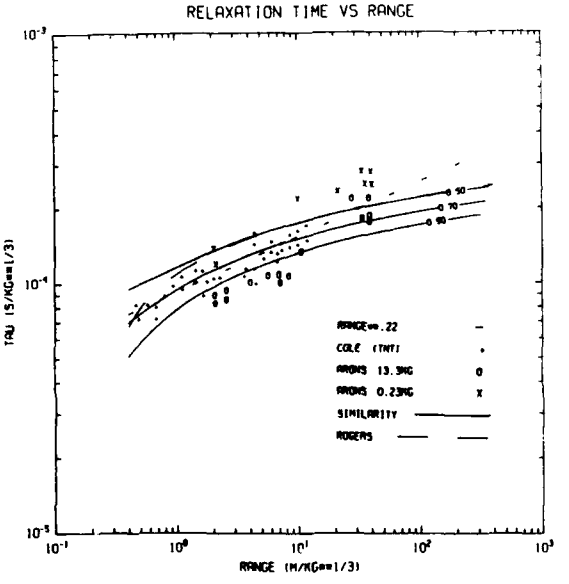

FIG. 4. Relaxation times τ_p: experimental values plotted as individual points, with theoretical curves taken from the empirical power law (1); from Eqs. (17) and (32) of the current theory, and from Rogers' theory.[2]

One possibility is depth variation of ambient pressure (or other parameters) neglected here. Effects of environmental variation would emerge supposedly at long ranges; this is, in fact, where theory and data begin to disagree concerning the behavior of the relaxation time.

VIII. SUMMARY

The nonlinear progressive wave equation (NPE) is an approximation to the Euler equations for nonlinear compressional waves in an inviscid fluid and, in fact, is the time domain equivalent to the parabolic equation (PE) when nonlinearity is omitted. In spherical symmetry, the NPE possesses a similarity solution that accounts for the following basic features of spherical shock waves generated in underwater explosions: (1) an approximate power law relation between shock overpressure and range; (2) shock relaxation time increasing roughly as a power law for approximately 1 decade in range near the source; and (3) pressure–time profiles resembling exponential falloff from the shock peak. As in a previous semiempirical similarity theory,[2] two free constants determine the solution. In the present theory, they are the overpressure at an initial range point, and the constant of integration α in Eq. (13). For plane waves, the theory predicts N wave shock solutions with peak overpressure varying as the inverse square root of the elapsed time and relaxation time varying directly as the square root of the time. Both of these lead to approximate power law variation with range. Only one free parameter is available for plane waves: the shock strength at a given range.

For discrete nonlinear pulses with or without shocks, the present theory predicts an integral of the motion given in Eq. (27) for solutions $s(r,t)$. In Eq. (29), the theory also demonstrates that this integral is a generalization of the linear impulse integral (7).

Discrepancies between the current theory and data are likely due to four assumptions made here to simplify the solution. First is the reduction of the fluid equations to a first-order nonlinear wave equation; second is the neglect of cubic and higher-order terms in the density perturbation; third is the assumption of self-similarity; and fourth is the assumption of a homogeneous medium ahead of the shock. One is assured that in the early phases of shock wave development (e.g., in explosive energy release or passage of a supersonic projectile) only the fourth is reasonable. The degree to which the current theory describes experimental results in later stages is then a statement about the dying out of transients and the progression toward a final state described by self-similarity.

ACKNOWLEDGMENTS

This work was supported by the Defense Nuclear Agency and the Office of Naval Research.

[1]P. H. Rogers and J. H. Gardner, "Propagation of Sonic Booms in the Thermosphere," J. Acoust. Soc. Am. 67, 78–91 (1980).
[2]P. H. Rogers, "Weak Shock Solution for Underwater Explosive Shock Waves," J. Acoust. Soc. Am. 62, 1412–1419 (1977).

[3]R. H. Cole, *Underwater Explosions* (Princeton U. P., Princeton, NJ, 1948).
[4]A. B. Arons, "Underwater Explosion Shock Wave Parameters at Large Distances from the Charge," J. Acoust. Soc. Am. **26**, 343–345 (1954).
[5]L. I. Sedov, *Similarity and Dimensional Methods in Mechanics*, English translation, edited by M. Holt (Academic, New York, 1959).
[6]W. D. Hayes and R. F. Probstein, *Hypersonic Flow Theory*, (Academic, New York, 1966).
[7]B. E. McDonald and W. A. Kuperman, "Time Domain Formulation for Pulse Propagation Including Nonlinear Behavior at a Caustic," J. Acoust. Soc. Am. **81**, 1406–1417 (1987).
[8]B. E. McDonald and W. A. Kuperman, "Time-Domain Solution of the Parabolic Equation Including Nonlinearity," Comput. Math. Appl. **11**, 843–851 (1985).
[9]F. D. Tappert, "The Parabolic Approximation Method," in *Wave Propagation and Underwater Acoustics*, Lecture Notes in Physics, Vol. 70, edited by J. B. Keller and J. S. Papadakis (Springer, New York, 1977), pp. 224–287.
[10]W. D. Hayes, *Gasdynamic Discontinuities* (Princeton U. P., Princeton, NJ, 1960).
[11]G. B. Whitham, *Linear and Nonlinear Waves* (Wiley, New York, 1974).
[12]Y. V. Petukhov, "Interpretation of the Anomalous Behavior of the Pressure Waveform from an Underwater Explosive Source," Sov. Phys. Acoust. **29**, 142–144 (1983).

AD-A203285

Unclassified
SECURITY CLASSIFICATION OF THIS PAGE

2

REPORT DOCUMENTATION PAGE

1a. REPORT SECURITY CLASSIFICATION Unclassified	1b. RESTRICTIVE MARKINGS DTIC FILE COPY
2a. SECURITY CLASSIFICATION AUTHORITY	3. DISTRIBUTION/AVAILABILITY OF REPORT Distribution Unlimited; approved for public release.
2b. DECLASSIFICATION/DOWNGRADING SCHEDULE	
4. PERFORMING ORGANIZATION REPORT NUMBER(S) JA 322:076:88, NORDA-216	5. MONITORING ORGANIZATION REPORT NUMBER(S)
6. NAME OF PERFORMING ORGANIZATION JASA	7a. NAME OF MONITORING ORGANIZATION Naval Ocean Research and Development Activity
6c. ADDRESS (City, State, and ZIP Code)	7b. ADDRESS (City, State, and ZIP Code) Stennis Space Center, MS 39529
8a. NAME OF FUNDING/SPONSORING ORGANIZATION / 8b. OFFICE SYMBOL (If applicable)	9. PROCUREMENT INSTRUMENT IDENTIFICATION NUMBER
8c. ADDRESS (City, State, and ZIP Code)	10. SOURCE OF FUNDING NOS. PROGRAM ELEMENT NO. / PROJECT NO. / TASK NO. / WORK UNIT NO.

11. TITLE (Include Security Classification)
Similarity solution for low Mach number spherical shocks

12. PERSONAL AUTHOR(S)
B.E. McDonald and J. Ambrosiano

13a. TYPE OF REPORT	13b. TIME COVERED	14. DATE OF REPORT (Yr., Mo., Day)	15. PAGE COUNT
Journal Article	From ____ To ____	1988	6

16. SUPPLEMENTARY NOTATION

17. COSATI CODES			18. SUBJECT TERMS (Continue on reverse if necessary and identify by block number)
FIELD	GROUP	SUB. GR	

19. ABSTRACT (Continue on reverse if necessary and identify by block number)

A nonlinear progressive wave equation (NPE) describes the evolution of a low Mach number shock wave. The NPE is the nonlinear time domain counterpart of the frequency domain linear parabolic wave equation (PE) for small angle propagation. The NPE is spherical symmetry admits a similarity solution that specifies both the shape of the pulse and the shock strength as a function of range. For finite amplitude spherical waves whether self-similar or not, the theory predicts constancy of an impulse integral corresponding to that of linear theory. For the self-similar waves, theory and available data are in qualitative agreement in the following areas: (1) The shock strength decreases with range as an approximate power law; (2) the temporal

20. DISTRIBUTION/AVAILABILITY OF ABSTRACT	21. ABSTRACT SECURITY CLASSIFICATION
UNCLASSIFIED UNLIMITED ☐ SAME AS RPT ☒ DTIC USERS ☐	Unclassified
22a. NAME OF RESPONSIBLE INDIVIDUAL B.E. McDonald	22b. TELEPHONE NUMBER (Include Area Code) (88) 297-5522
22c. OFFICE SYMBOL 322	

DD FORM 1473, 83 APR — EDITION OF 1 JAN 73 IS OBSOLETE

Unclassified
SECURITY CLASSIFICATION OF THIS PAGE

19. Abstract (Continuation)

behavior of the solution at fixed range is a shock discontinuity followed by a roughly exponential decay; and (3) the effective relaxation time behind the shock is in reasonable agreement with data for slightly more than the first decade in range.